Three Phase Dual Active Bridges with Integrated Series Inductance using 10-kV SiC MOSFETs for Medium Voltage Grid Applications

1st Roderick A. Gomez
Department of Electrical Engineering
University of Arkansas
Fayetteville, AR, USA
ragomezj@uark.edu

2nd David A. Porras
Department of Electrical Engineering
University of Arkansas
Fayetteville, AR, USA
daporras@uark.edu

3rd German Oggier
Grupo de Electronica Aplicada (GEA)
Universidad de Rio Cuarto (UNRC)
Rio Cuarto Cordoba, Argentina
goggier@ieee.org

4rd Juan Balda
Department of Electrical Engineering
University of Arkansas
Fayetteville, AR, USA
jbalda@uark.edu

5th Yue Zhao
Department of Electrical Engineering
University of Arkansas
Fayetteville, AR, USA
yuezhao@uark.edu

***Abstract*— The advancement of high blocking capacity silicon carbide (SiC) power modules enables the development of next generation highly efficient and highly power dense conversion units for medium voltage applications without implementing complex multilevel topologies. This paper presents the design and testing of a 150-kW medium-voltage (MV) three-phase dual active bridge (DAB) using 10-kV Wolfspeed SiC MOSFETs for MV AC and DC grid applications. The DAB is designed for a MV of 5 kVdc and a low voltage of 400 Vdc. A high efficiency, low parasitic capacitance 10-kHz three-limb three phase transformer with integrated leakage inductance for rated power transfer is used to provide galvanic isolation. The proposed prototype was experimentally validated up to 45 kW with an input voltage up to 4 kV. Experimental voltage and current waveforms are provided for each operating condition.**

Keywords—Silicon Carbide (SiC), Dual Active Bridge (DAB), Solid state transformer, medium voltage, medium frequency transformer, three phase converter.

I. INTRODUCTION

Wide bandgap silicon carbide (SiC) semiconductors have propelled the evolution of power electronics conversion units characterized by high efficiency, high power density, and faster switching frequencies [1], [2]. SiC power modules have disrupted the electric vehicle industry with highly efficient traction inverters and onboard charges [3]-[5] while entering other markets [6]-[8] at an accelerated pace. These industries exploit the well refined SiC MOSFETs ranging from a few couple of volts to 1700 V. Nonetheless, the medium voltage grid connected market is hindered by the need to employ highly complex multilevel structures with these well-developed SiC power modules to achieve a power conversion unit capable of interfacing medium or high voltages [9], [10]. As a result, attention has been paid to the development of high voltage SiC power modules [11], [12].

High blocking voltage wide bandgap SiC MOSFET devices have allowed designers to reach MV levels while reducing the complexity seen on modular multilevel converter (MMC) topologies [13], [14] and reducing the number of cells needed for cascaded H-bridge (CHB) topologies [15]. The proposed 4.16 kVac solid state transformer presented in [16] and the 7kV/400V DC transformer in [17] demonstrate the feasibility of MV power modules for simple single level power conversion units while the work presented in [18] and [19] validate MV power modules application in multilevel converters. Furthermore, these next generation SiC-based devices have the advantages of lower on-state resistance and faster switching frequencies resulting in reduced weight and size of the magnetic components, thus enabling different MV applications such as medium voltage EV charging stations, energy storage, and medium voltage multimegawatt dc and ac grid [20]-[21].

The work in [22] compared a modular multilevel dc converter (M2DC) and the DAB used for power conversion from an HVDC grid to an MVDC grid in terms of efficiency, amount of semiconductor devices, and cost of capacitive storage and magnetic components. This study concluded that the DAB system features an efficiency between 98.9 % and 99.2 %. However, the M2DC requires many semiconductors, resulting in investment costs for an M2DC at least a factor of three higher. Besides, they need a similar number of magnetic components compared to the soft-switching DAB system. Moreover, the work in [23] evaluates isolated DC/DC converter topologies. It concludes that the DABs, particularly the three-phase option, present lower switching losses than other possibilities due to

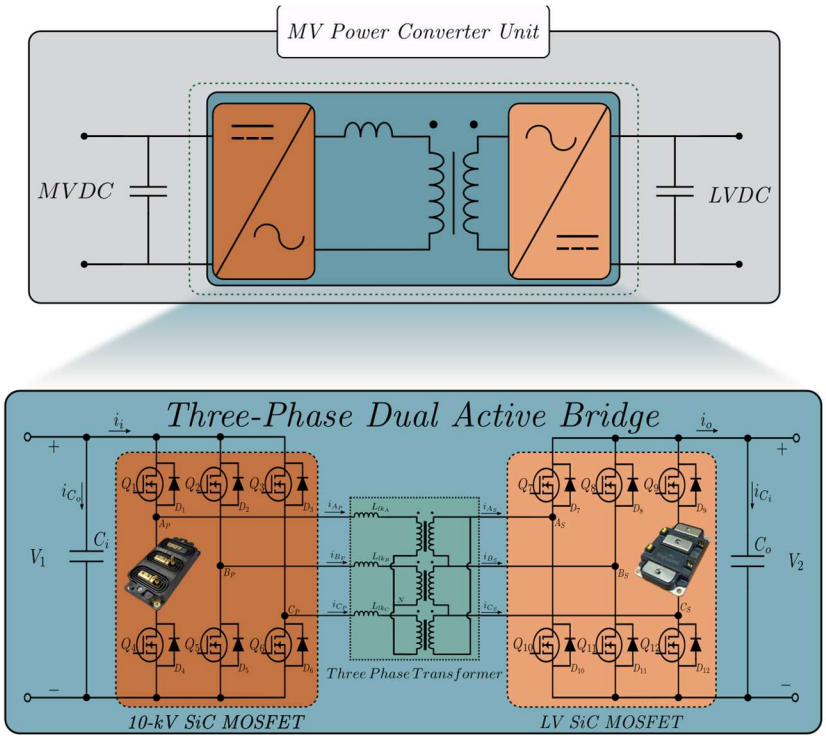

Fig. 1. Medium voltage DC transformer schematic using a three-phase dual-active-bridge topology.

their natural capability of achieving ZVS at the turn-on. Furthermore, this characteristic is obtained over a wide operating range without drastically increasing the control system complexity [24]. The advantage of the DAB poses itself as one of the most promising isolated bidirectional DC/DC converters to meet the challenge of the future power system of smart-grid technologies at the medium voltage level as presented and validated in [16], [17]. Subsequently, this paper presents a high power DC transformer using 3rd generation 10 kV SiC as an isolated DC building block for medium voltage power conversion applications. The work presented utilizes a three-phase DAB with a medium frequency (MF) three-limb three phase transformer with integrated series leakage inductance to meet maximum power transfer requirements at a lower volume and weight. The proposed converter is designed with an input voltage of 5 kVdc and an output voltage of 400 Vdc, resulting in a power rating of 150 kW. Table I summarized the converter specifications.

II. Three Phase Dual Active Bridge with Integrated Magnetics

The three-phase DAB (TPDAB) is a well-known topology with the benefits of high-power density and reduced current

TABLE I
THREE-PHASE DAB DC/DC CONVERTER SPECIFICACTIONS

Parameter	Value	Unit
Rated Power	150	kVA
Input Voltage	5	kV
Output Voltage	400	V
Switching Frequency	10	kHz
Series Inductance	920	μH

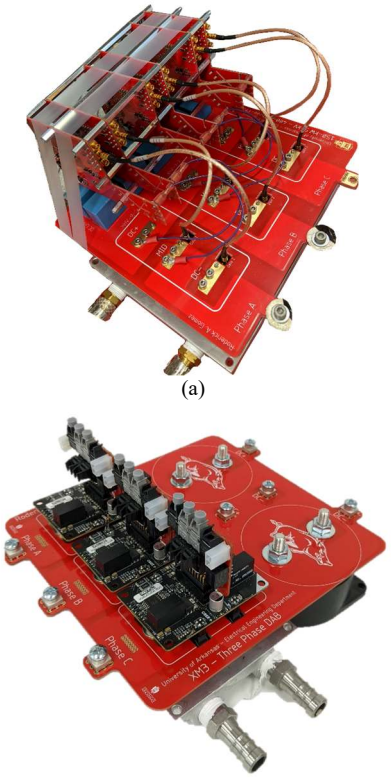

(a)

(b)

Fig 2. (a) 10 kV SiC power module three-phase PCB MV bridge and (b) XM3 SiC power module three-phase heavy copper PCB LV bridge.

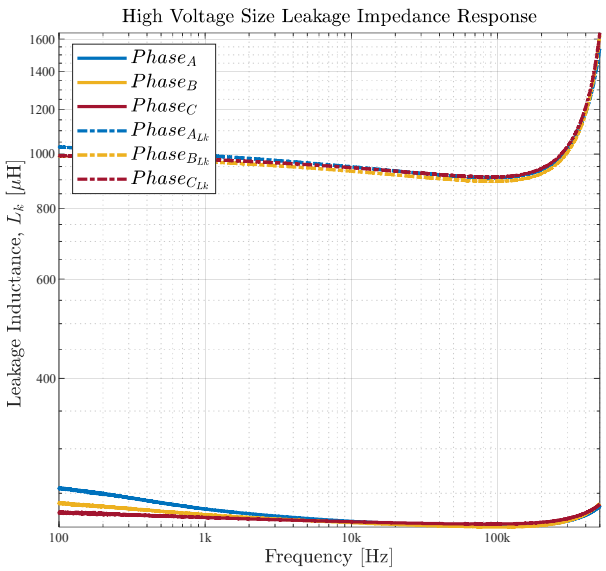

Fig. 3. Impedance response as seen from the primary high voltage side.

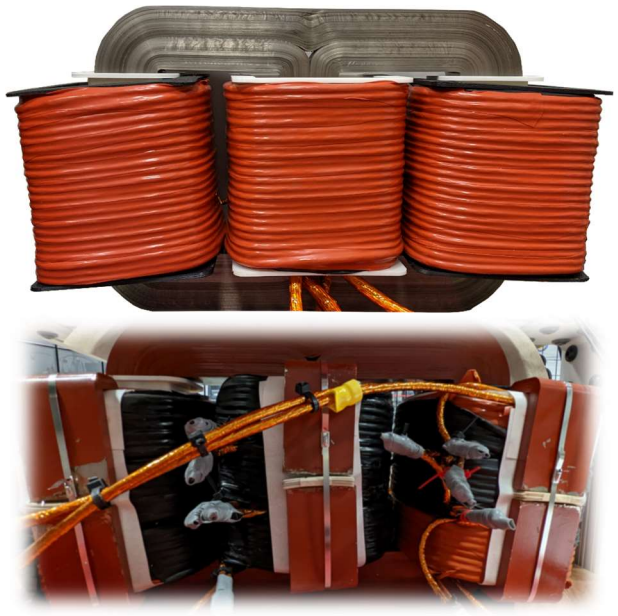

Fig. 4. Integrated series inductance MF transformer

stresses on the semiconductor devices compared to the single-phase version [24], [25], demonstrating the potential of the TPDAB to be employed in high power medium voltage level applications where utilization have been already reported in [16]. As a result, the three-phase DAB was chosen for the medium voltage medium frequency DC transformer presented in this work.

A. MV and LV Power Stages

Fig. 1 shows the TPDAB topology for the proposed DC transformer. The MV side three-phase bridge is composed of 3rd generation 10 kV XHV-9 SiC MOSFETs from Wolfspeed. The MV power stage was designed using PCB bus bar with increase FR4 core thickness to ensure electric isolation between the DC+ plane and the DC- plane. Additionally, reinforced solder mask coating was applied to the PCB bus board. The gates of the 10 kV SiC MOSFETs are driven by a single switch position MV gate driver connected using short high-frequency mini coaxial cables. Off-the-shelf isolated power supplies with a coupling capacitance < 5pF and isolation up to 15 kV are used to power each individual gate driver. Moreover, control signals for each of the gate drivers are fed through fiber optic to avoid any EMI interference. Fig. 2a shows the built MV side power stage.

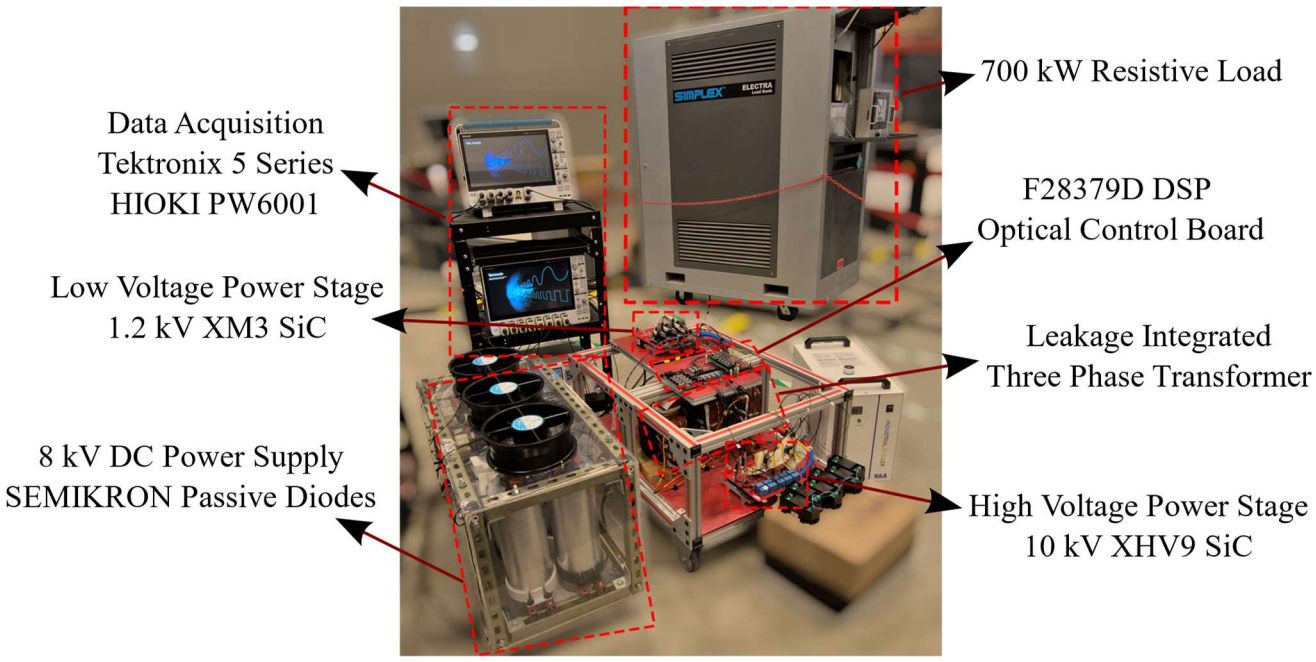

Fig. 5. High voltage, high power experimental test setup at NCREPT facilities.

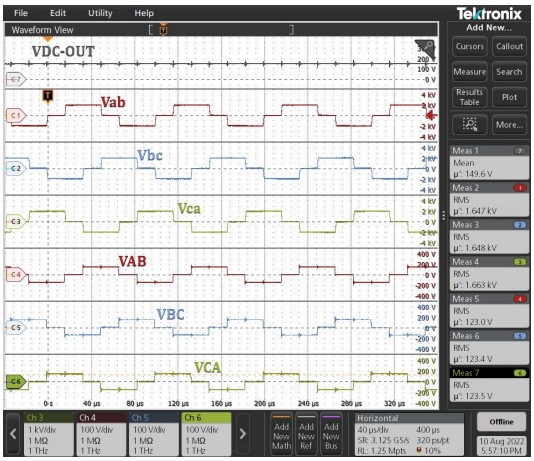

(a)

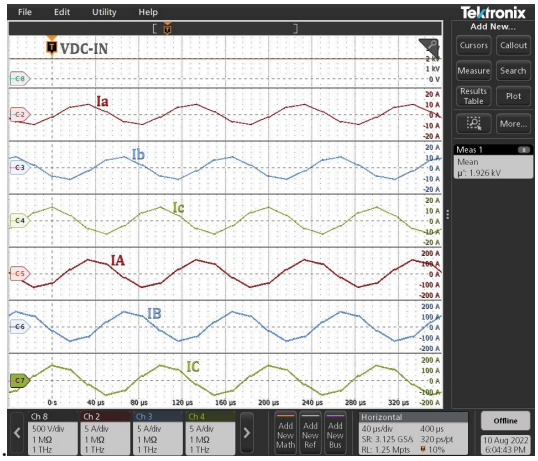

(b)

Fig 6. (a) Line voltages waveforms and (b) line currents for each phase at 2 kV input voltage.

The low voltage (LV) power stage is built with 1.2-kV, 450A XM3 SiC MOSFET from Wolfspeed. Like the MV power stage, the LV side three-phase bridge was designed using heavy cooper PCB with specifications to meet minimum creepage and clearance requirements. Each LV power module is controlled by commercial Wolfspeed gate drivers with a custom-made optical transceiver to feed control signals using fiber optic cables. LV power stage is illustrated in Fig. 2b. The control of both bridges is done using a custom-made optical transceiver board for an F28379D DSP control card.

B. Medium Frequency Three-Phase Transformer

Ribbon-based soft-magnetic materials like amorphous and nanocrystalline have been demonstrated to yield better efficiency and power densities than materials like ferrite [26], [27]. Moreover, these materials provide easy manufacturing process for custom cores which allows for a single-core design for the three-phase transformer to be implemented with optimal efficiency, volume, and cost. Thus, the work presented in this paper employs a three-limb single core transformer for galvanic isolation whose design and testing were reported in [28]. Improvement in the power density of the transformer and DAB was achieved by integrating the series leakage inductance required for maximum power transfer by including an auxiliary

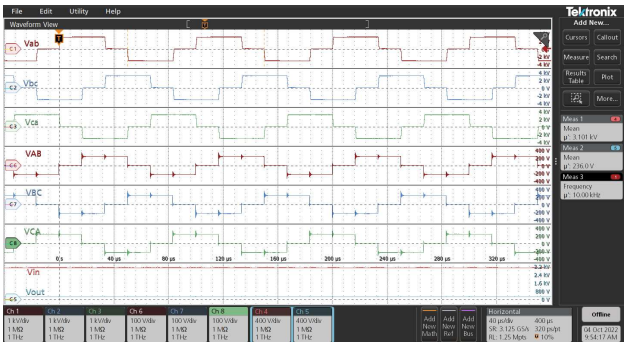

(a)

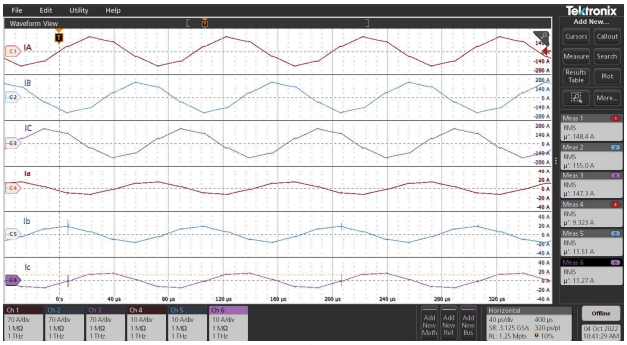

(b)

Fig 7. (a) Line voltages waveforms and (b) line currents for each phase at 2 kV input voltage.

leakage core on the MV winding. The impedance response presented in Fig. 3 validated the increase of leakage inductance seen from the primary side due to the integrated cores. Moreover, parasitic capacitance due to the high number of turns on the medium voltage windings needed to be addressed to avoid unwanted resonances on the phase voltages and currents. Winding arrangements procedures to mitigate these parasitic capacitances are outside the scope of this paper and stated in [29], where the reduction on current resonance for different winding arrangements were presented. Fig. 4 shows the designed single-core three-phase integrated leakage inductance MF transformer with low winding capacitance for the TPDAB.

[30] demonstrated that converter efficiency and soft-switching range is affected by the configuration of the MF transformer terminals. It has been shown in [31] and [32] that for the three-phase DAB, the wye-delta ($Y-\Delta$) configuration of the three-phase MF transformer yield higher efficiency and lower transformer volume when compared to Y-Y and Δ- Δ configurations. For these reasons, the built MF transformer was connected in $Y-\Delta$ for the TPDAB.

III. THREE PHASE DUAL ACTIVE BRIDGE EXPERIMENTAL RESULTS AND DISCUSSION

The three-phase DAB prototype was initially tested to verify proper operation at high voltages and low-power levels using a 6-kV Magna DC power supply and a Simplex Electra resistive load bank. The TPDAB was tested up to 4 kV at 10 kW output power in an open loop configuration. To validate the prototype at higher power levels, the TPDAB converter was tested at the National Center for Reliable Electric Power Transmission (NCREPT) at the University of Arkansas. For this experimental

validation, a three-phase ac-dc passive rectifier was built using high voltage 2.2 kV SEMIKRON single diode modules connected in series for passive rectification up to 7.5kVdc and 500 kVA. Then, the passive front end rectifier is connected to the NCREPT medium voltage bus which is driven by a three-phase variable-frequency, variable-voltage inverter (3VF), allowing for soft-start of the dc/dc converter. Experimental setup at NCREPT facilities is shown in Fig. 6. The data acquisition equipment consists of a Tektronix MSO58 and a MSO56 oscilloscope with THDP0200 and THDP0100 high voltage differential probes and PEM CWT MiniHF Rogowski Coils. A HIOKI PW6001 power analyzer monitors input and output dc currents and input and output dc voltages. To avoid damage to the power analyzer, a precision voltage divider was used to monitor the high input voltage.

The initial testing of the TPDAB was conducted at an input voltage of 2 kV with a load resistance of 1.28 Ω connected to the LV side. These operating conditions should output about 20 kW. Results waveforms of this experiment are shown in Fig. 6 where all line currents and line voltages waveforms are presented. Power analyzer measurements showed the converter yield an efficiency of about 99% with an output power of 20.2 kW. MV line voltages do not show any low or high frequency resonance due to any parasitic capacitance of the module or the transformer windings. Nonetheless, the line voltages made noticeable the low dv/dt of the 10 kV SiC when compared with the dv/dt of lower voltage MOSFETs. LV lines voltages showed a high frequency resonance that follows the turn-on transient of each module since each MOSFETs will form a resonance circuit between its output capacitance and the stray inductance causing an overshoot. All the line currents during the 2 kV did not exhibit any overshoot or resonance during turn-on or turn-off of the power modules. Further tests were conducted at an input voltage of 3 kV while keeping the load resistance constant at 1.28 Ω. The 3 kV experiment data is presented in Fig. 7 where the lines voltage and currents are presented yielding an efficiency of 98.9% at an output power of about 45 kW. All lines voltages for this operating condition showed similar behavior as previous experimental test. However, the MV line currents were displaying a small spike which may be attributed to the 60-degree phase shift used for the open loop experimental test since the leakage inductor would see a high voltage in a brief instant causing the spikes. Power analyzer measurements are presented in Fig. 8 for the 20 kW and 45 kW. Although LV line voltages for both experiments showed high frequency oscillations during the switching transients due to the MOSFETs output capacitance, MV line voltages and MV and LV line currents do not present oscillation of low frequency ringing during the step of the secondary voltage which it has been an issue for medium voltage transformer as reported in [16].

IV. Conclusion

This work illustrated the feasibility of MV SiC MOSFETs in MV applications to reduce the complexity of cascaded topologies aimed at MV distribution systems and even sub-transmission systems (e.g., 69 kV). It provides testing results of a 150-kW 10-kHz DC transformer realized using a three-phase dual-active-bridge topology. The presented prototype was tested under 20 kW and 45 kW load yielding an efficiency of about 98.8%. Furthermore, experimental line voltages and currents waveforms did not present any unwanted low frequency ringing because of high parasitic capacitance on the medium voltage windings, demonstrating the benefits of the measures taken to mitigate these capacitances. The designed DAB incorporated the concept of integrated magnetics to improve power density by eliminating the need for external series inductors which tend to increase the overall volume of the converter without compromising the transformer efficiency. Future work includes continuous testing of the dc/dc converter at higher power level >100 kW while opting to increase the switching frequency and input voltage level to evaluate possible drawbacks and improvements for a next generation of the presented medium voltage dc/dc converter.

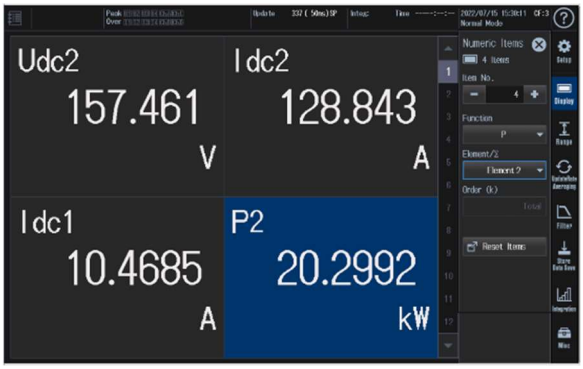

(a)

(b)

Fig 8. Power analyzer measurements at (a) 20 kW for the 2 kV input voltage experiment and (b) 45 kW for the 3 kV experimental test.

Acknowledgment

The authors are grateful about the financial support received from the NSF I/UCRC Grid-Connected Advanced Power Electronics Systems GR-20-04 under "All-SiC Medium Voltage Medium Frequency DC-DC Converter Project" and the Department of Energy financial support under "A reliable, Cost-Effective Transformerless Medium-Voltage Inverter for Grid Integration of Combined Solar and Energy Storage" Award DE-EE0008349. Testing for this project was conducted at the National Center for Reliable Electric Power Transmission (NCREPT), the University of Arkansas.

REFERENCES

[1] T. KIMOTO, “High-voltage SIC power devices for improved energy efficiency,” Proceedings of the Japan Academy, Series B, vol. 98, no. 4, pp. 161–189, 2022.

[2] J. W. Palmour et al., "Silicon carbide power MOSFETs: Breakthrough performance from 900 V up to 15 kV," 2014 IEEE 26th International Symposium on Power Semiconductor Devices & IC's (ISPSD), 2014, pp. 79-82, doi: 10.1109/ISPSD.2014.6855980.

[3] J. W. Palmour et al., "Silicon carbide power MOSFETs: Breakthrough performance from 900 V up to 15 kV," 2014 IEEE 26th International Symposium on Power Semiconductor Devices & IC's (ISPSD), 2014, pp. 79-82, doi: 10.1109/ISPSD.2014.6855980.

[4] J. Zhu, H. Kim, H. Chen, R. Erickson and D. Maksimović, "High efficiency SiC traction inverter for electric vehicle applications," 2018 IEEE Applied Power Electronics Conference and Exposition (APEC), 2018, pp. 1428-1433, doi: 10.1109/APEC.2018.8341204.

[5] B. Wu and S. Shi, "78 W Auxiliary Power Supply for 22-KW Drive Using 1700 V Silicon Carbide MOSFET," PCIM Asia 2020; International Exhibition and Conference for Power Electronics, Intelligent Motion, Renewable Energy and Energy Management, 2020, pp. 1-4.

[6] J. W. Palmour, "Silicon carbide power device development for industrial markets," 2014 IEEE International Electron Devices Meeting, 2014, pp. 1.1.1-1.1.8, doi: 10.1109/IEDM.2014.7046960.

[7] X. She, A. Q. Huang, Ó. Lucía and B. Ozpineci, "Review of Silicon Carbide Power Devices and Their Applications," in IEEE Transactions on Industrial Electronics, vol. 64, no. 10, pp. 8193-8205, Oct. 2017, doi: 10.1109/TIE.2017.2652401.

[8] J. Wu et al., "Impact of SiC MOSFET on PV Inverter," 2018 IEEE Energy Conversion Congress and Exposition (ECCE), 2018, pp. 1853-1860, doi: 10.1109/ECCE.2018.8558284.

[9] B. Hu et al., "A Survey on Recent Advances of Medium Voltage Silicon Carbide Power Devices," 2018 IEEE Energy Conversion Congress and Exposition (ECCE), 2018, pp. 2420-2427, doi: 10.1109/ECCE.2018.8558451.

[10] V. Pala et al., "10 kV and 15 kV silicon carbide power MOSFETs for next-generation energy conversion and transmission systems," 2014 IEEE Energy Conversion Congress and Exposition (ECCE), 2014, pp. 449-454, doi: 10.1109/ECCE.2014.6953428.

[11] A. Q. Huang, Q. Zhu, L. Wang and L. Zhang, "15 kV SiC MOSFET: An enabling technology for medium voltage solid state transformers," in CPSS Transactions on Power Electronics and Applications, vol. 2, no. 2, pp. 118-130, 2017, doi: 10.24295/CPSSTPEA.2017.00012.

[12] C. M. DiMarino, B. Mouawad, C. M. Johnson, D. Boroyevich and R. Burgos, "10-kV SiC MOSFET Power Module With Reduced Common-Mode Noise and Electric Field," in IEEE Transactions on Power Electronics, vol. 35, no. 6, pp. 6050-6060, June 2020, doi: 10.1109/TPEL.2019.2952633.

[13] M. S. Diab and X. Yuan, "A Modular Quasi-Multilevel Converter using 10kV SiC MOSFETs for Medium-Voltage Cable-Fed Variable-Speed Motor Drives," 2021 IEEE 12th Energy Conversion Congress & Exposition - Asia (ECCE-Asia), 2021, pp. 781-786, doi: 10.1109/ECCE-Asia49820.2021.9479096.

[14] S. Madhusoodhanan et al., "Comparative evaluation of 15 kV SiC IGBT and 15 kV SiC MOSFET for 3-phase medium voltage high power grid connected converter applications," 2016 IEEE Energy Conversion Congress and Exposition (ECCE), 2016, pp. 1-8, doi: 10.1109/ECCE.2016.7854933.

[15] H. Mhiesan, C. Farnell, R. McCann and A. Mantooth, "Evaluation of a Medium-Voltage Grid-Tied Cascaded H-Bridge for Energy Storage Systems Using SiC Switching Devices," 2018 IEEE Electronic Power Grid (eGrid), 2018, pp. 1-5, doi: 10.1109/eGRID.2018.8598683.

[16] A. Anurag, S. Acharya, S. Bhattacharya, T. R. Weatherford and A. A. Parker, "A Gen-3 10-kV SiC MOSFET-Based Medium-Voltage Three-Phase Dual Active Bridge Converter Enabling a Mobile Utility Support Equipment Solid State Transformer," in IEEE Journal of Emerging and Selected Topics in Power Electronics, vol. 10, no. 2, pp. 1519-1536, April 2022, doi: 10.1109/JESTPE.2021.3069810.

[17] D. Rothmund, T. Guillod, D. Bortis and J. W. Kolar, "99% Efficient 10 kV SiC-Based 7 kV/400 V DC Transformer for Future Data Centers," in IEEE Journal of Emerging and Selected Topics in Power Electronics, vol. 7, no. 2, pp. 753-767, June 2019, doi: 10.1109/JESTPE.2018.2886139.

[18] D. N. Dalal et al., "Demonstration of a 10 kV SiC MOSFET based Medium Voltage Power Stack," 2020 IEEE Applied Power Electronics Conference and Exposition (APEC), 2020, pp. 2751-2757, doi: 10.1109/APEC39645.2020.9124441.

[19] D. N. Dalal et al., "Demonstration of a 10 kV SiC MOSFET based Medium Voltage Power Stack," 2020 IEEE Applied Power Electronics Conference and Exposition (APEC), 2020, pp. 2751-2757, doi: 10.1109/APEC39645.2020.9124441.

[20] R. Chen et al., "10 kV SiC MOSFET Based Medium Voltage Power Conditioning System for Asynchronous Microgrids," in IEEE Access, vol. 10, pp. 73294-73308, 2022, doi: 10.1109/ACCESS.2022.3189003.

[21] R. Chen et al., "10 kV SiC MOSFET Based Medium Voltage Power Conditioning System for Asynchronous Microgrids," in IEEE Access, vol. 10, pp. 73294-73308, 2022, doi: 10.1109/ACCESS.2022.3189003.

[22] S. P. Engel, M. Stieneker, N. Soltau, S. Rabiee, H. Stagge and R. W. De Doncker, "Comparison of the Modular Multilevel DC Converter and the Dual-Active Bridge Converter for Power Conversion in HVDC and MVDC Grids," in IEEE Transactions on Power Electronics, vol. 30, no. 1, pp. 124-137, Jan. 2015, doi: 10.1109/TPEL.2014.2310656.

[23] L. Tarisciotti, A. Costabeber, C. Linglin, A. Walker and M. Galea, "Evaluation of isolated DC/DC converter topologies for future HVDC aerospace microgrids," 2017 IEEE Energy Conversion Congress and Exposition (ECCE), 2017, pp. 2238-2245, doi: 10.1109/ECCE.2017.8096437

[24] “Comparative analysis of single and three-phase dual active bridge bidirectional DC-DC converters -IEEE Conference Publication.” https://ieeexplore.ieee.org/document/4813089 (accessed Aug. 10, 2020).

[25] H. van Hoek, M. Neubert, A. Kroeber, and R. W. de Doncker, “Comparison of a single-phase and a three-phase dual active bridge with low-voltage, high-current output,” 2012, doi: 10.1109/ICRERA.2012.6477466.

[26] W. Shen, F. Wang, D. Boroyevich and C. W. Tipton IV, "High-Density Nanocrystalline Core Transformer for High-Power High-Frequency Resonant Converter," in IEEE Transactions on Industry Applications, vol. 44, no. 1, pp. 213-222, Jan.-feb. 2008, doi: 10.1109/TIA.2007.912726.

[27] M. S. Rylko, K. J. Hartnett, J. G. Hayes and M. G. Egan, "Magnetic Material Selection for High Power High Frequency Inductors in DC-DC Converters," 2009 Twenty-Fourth Annual IEEE Applied Power Electronics Conference and Exposition, 2009, pp. 2043-2049, doi: 10.1109/APEC.2009.4802955.

[28] R. A. G. Jimenez, G. G. Oggier, R. A. Fantino, J. C. Balda and Y. Zhao, "Design of Nanocrystalline Medium-Voltage Medium-Frequency Three-Phase Transformers for Grid-Connected Applications," 2021 IEEE Energy Conversion Congress and Exposition (ECCE), 2021, pp. 1142-1148, doi: 10.1109/ECCE47101.2021.9595466.

[29] R. A. G. Jimenez, G. G. Oggier, D. P. Fernandez and J. C. Balda, "Analysis of Current Resonances due to Winding Parasitic Capacitances in Medium-Voltage Medium-Frequency Transformers," 2022 IEEE Applied Power Electronics Conference and Exposition (APEC), 2022, pp. 939-943, doi: 10.1109/APEC43599.2022.9773427.

[30] R.O. Núñez, G.G. Oggier, F. Botterón, G.O. García, "A comparative study of Three–Phase Dual Active Bridge Converters for renewable energy applications", Sustainable Energy Technologies and Assessments, Volume 23, 2017, Pages 1-10, ISSN 2213-1388, https://doi.org/10.1016/j.seta.2017.07.004.

[31] K. Jin and C. Liu, "A Novel PWM High Voltage Conversion Ratio Bidirectional Three-Phase DC/DC Converter With Y–Δ Connected Transformer," in IEEE Transactions on Power Electronics, vol. 31, no. 1, pp. 81-88, Jan. 2016, doi: 10.1109/TPEL.2015.2397455.

[32] N. H. Baars, J. Everts, C. G. E. Wijnands and E. A. Lomonova, "Performance Evaluation of a Three-Phase Dual Active Bridge DC–DC Converter With Different Transformer Winding Configurations," in IEEE Transactions on Power Electronics, vol. 31, no. 10, pp. 6814-6823, Oct. 2016, doi: 10.1109/TPEL.2015.2506703.